Journal of Electronic Materials (2023) 52:1590–1598
https://doi.org/10.1007/s11664-022-10133-8

ORIGINAL RESEARCH ARTICLE

Dual-Band Quasi-Isotropic Dielectric Resonator-Based Filtering Antenna for IoT Applications

Abhimanyu Yadav[1] · **Manish Tiwari**[1] · **Anand Sharma**[1]

Received: 10 October 2022 / Accepted: 28 November 2022 / Published online: 21 December 2022

Abstract

In this work, a dual dielectric resonator antenna (DRA) oriented in opposite directions is designed and analyzed. The unique feature of the proposed antenna is to provide dual-band filtering characteristics with a quasi-isotropic radiation pattern. The upper cylindrical ceramic is fed by the combination of a conformal strip and a circular patch, while the lower one is fed by a circular aperture. The proposed feeding mechanism produces $HEM_{11\delta}$ and $HEM_{12\delta}$ modes inside the ceramic material at 2.8 GHz and 5.4 GHz, respectively, providing a dual-band response. The proposed radiator has two main features: (i) the arrangement of the ceramic-based radiator creates radiation nulls at 5.8 GHz, 4.8 GHz, 3.5 GHz and 2 GHz, which provides the filtering response, and (ii) the opposite orientation of the dual ceramic produces quasi-isotropic radiation features. Experimental measurements confirm its operation in the frequency ranges of 2.48–3.3 GHz and 5.21–5.48 GHz. Maximum rejection is about −20 dBi in both frequency bands, while the passband gain is about 5.0 dBi. These radiation characteristics make the proposed antenna suitable for the WLAN (2.5 GHz/5.15 GHz) frequency band.

Keywords Dielectric resonator antenna · filtenna · quasi-isotropic radiation pattern

Introduction

In the current world of the Internet of Things (IoT), communication among a number of wireless nodes is necessary. In general, the orientation and relative position of the various wireless nodes is not known. Antennas with quasi-isotropic radiation behavior are widely used to serve this purpose.[1] These antennas radiate uniformly in all directions. Another important requirement of antennas used for IoT applications is miniaturization. This can be achieved using the concept of filtennas. Antennas integrated with a filtering response eliminate the need for a bandpass filter in the front end of the radio frequency (RF) system, which in turn reduces the overall size of the device.[2] In the literature, various researchers have dealt separately with antenna design using a filtering response and a quasi-isotropic radiation pattern. There are two approaches in general which are used to obtain the filtering characteristics: the filter synthesis approach[3,4] and the antenna fusion approach.[5,6] In the first technique, the filter is realized first and the radiator is implemented at the end of the filtering structure. Dhwaj et al. proposed a dual-resonant cavity design with electric coupling between them, which acts as a bandpass filter. At the end, a radiator is added.[3] Similarly, Mao et al. proposed a U-slot-loaded patch antenna which achieves bandpass filtering characteristics by using the concept of filter synthesis.[4] The problem associated with this approach is the high insertion loss and poor radiation characteristics. Another approach, antenna fusion, focuses on the antenna design, and filtering characteristics are obtained with the assistance of a radiation null concept. Hu et al. presented a dielectric resonator antenna (DRA) fed by a hybrid metallic ring along with a shorting pin, which provides radiation nulls at 3.8 GHz, 3.1 GHz, 2.6 GHz and 1.8 GHz.[5] Pan et al. reported a dual-strip-loaded microstrip line-fed rectangular DRA, which provides radiation nulls at 1.6 GHz and 2.3 GHz.[6]

The quasi-isotropic radiation pattern provides approximately uniform power levels throughout the space.

✉ Anand Sharma
anandsharma@mnnit.ac.in

Abhimanyu Yadav
abhimanyuy694@gmail.com

Manish Tiwari
mtiwari@mnnit.ac.in

[1] Department of Electronics and Communication Engineering, Motilal Nehru National Institute of Technology Allahabad, Prayagraj, Uttar Pradesh, India

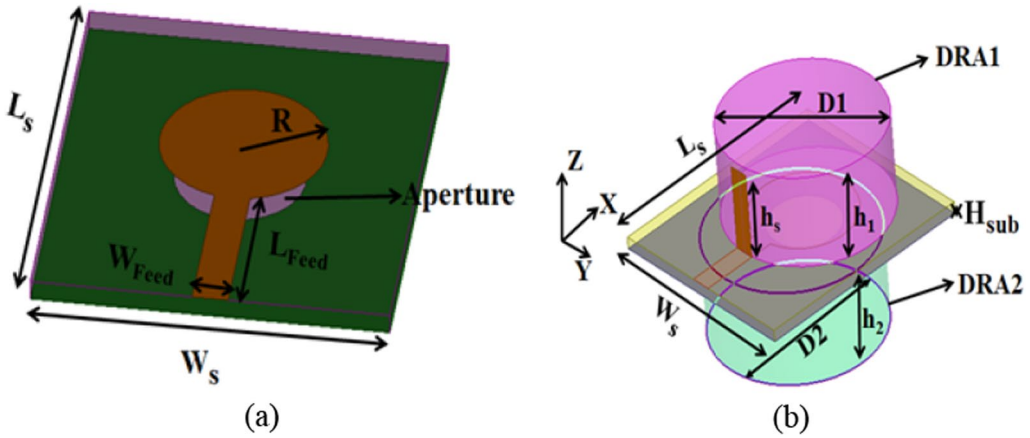

Fig. 1 Geometric layout of designed filtenna. (a) Feeding structure, (b) 3D view. LS = 35.0 mm; WS = 30.0 mm; HSub = 1.6 mm; D1 = 25.0 mm; D2 = 26.0 mm; h1 = 12.5 mm; h2 = 13.0 mm; LFeed = 20.0 mm; WFeed = 3.0 mm; R = 7 0.0 mm; hs = 11.5 mm.

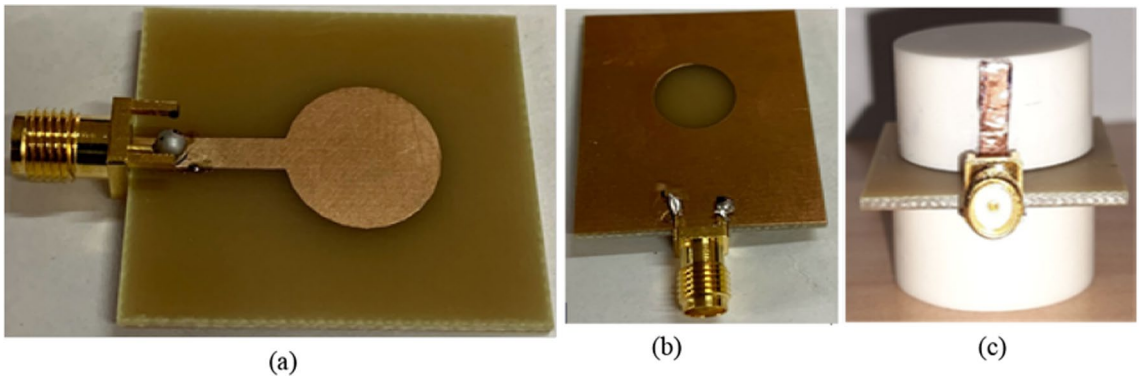

Fig. 2 Prototype of designed filtenna. (a) Top view of feeding structure, (b) bottom view of feeding structure, (c) 3D view.

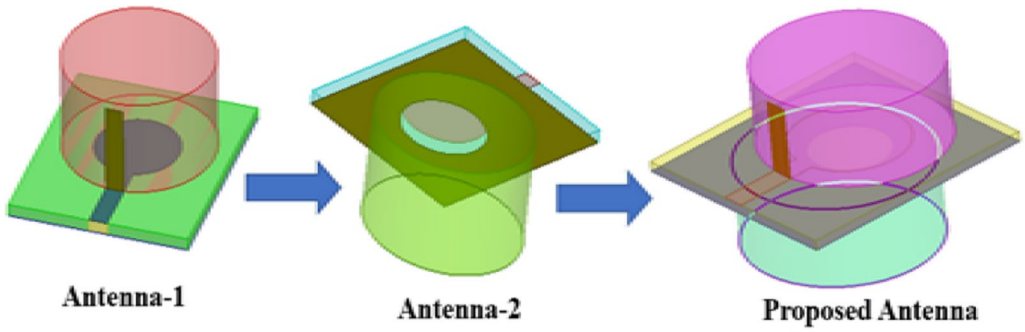

Fig. 3 Step-by-step design process for the proposed antenna.

Therefore, these antennas are widely used in IoT applications. To create this radiation pattern, different techniques are available in the literature. For instance, arranging the number of directional radiators in a circular manner provides a quasi-isotropic radiation pattern.[7] However, this makes the radiating structure more bulky and difficult to use in a

practical scenario. Another important approach for creating a quasi-isotropic radiation pattern is to combine a magnetic dipole with an electric dipole at a certain frequency. Pan et al. proposed a quasi-isotropic DRA using this concept. They combined a metallic probe (electric dipole) with a hybrid electromagnetic $(HEM)_{11\delta}$ mode inside the DRA (magnetic dipole) at 2.4 GHz.[8] Another article reported on a DRA with combined features, i.e. both filtering and quasi-isotropic radiation characteristics. An aperture-coupled cylindrical DRA (CDRA) with a small ground plane was used for that purpose.[9] However, the above-reported devices are single-band antennas, and it is clear that dual-band DRA with both filtering response and quasi-isotropic radiation is missing in the literature. In this article, two modes, $HEM_{11\delta}$ and $HEM_{12\delta}$, are created in a special arrangement of a cylindrical ceramic at 3.0 GHz and 5.4 GHz, which thus supports dual-band characteristics. The dual cylindrical ceramic is placed on the upper and lower parts of the substrate, which is fed by a circular patch with a conformal strip and circular aperture, respectively. Filtering characteristics are obtained by creating radiation nulls at 5.8 GHz, 4.8 GHz, 3.5 GHz and 2 GHz with the help of a feeding structure. To provide an in-depth understanding of this design, the remainder of this article is arranged as follows: (II) geometry of the antenna structure and its operating principle; (III) step-by-step analysis; (IV) measured outcomes and performance comparison; and (V) conclusion.

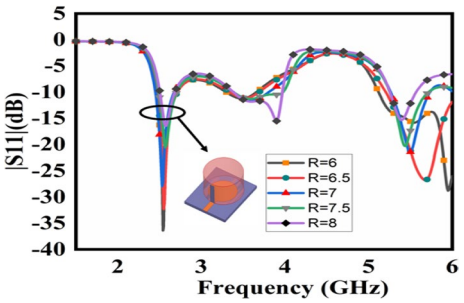

Fig. 4 |S11| variation due to change in radius of circular metallic patch (R).

Geometric Layout of Proposed Quasi-Isotropic Filtering Radiator

The geometric layout of the proposed filtenna is presented in Fig. 1. The feeding structure is displayed in Fig. 1a, and the 3D view of the designed filtenna is shown in Fig. 1b. DRA-1 and DRA-2 are the cylindrical alumina ceramics (tan $\delta = 0.02$, $\varepsilon_{Alumina} = 9.8$). DRA-1 is fed by a circular patch along with a conformal strip and placed on the upper part of the substrate. DRA-2 is fed by a circular aperture and placed on the lower part of the substrate. The radius of the aperture (Ra) is 5.5 mm. The complete feeding structure has been etched from the FR-4 substrate (tan $\delta = 0.002$, $\varepsilon FR\text{-}4 = 4.4$). Figure 2 presents a picture of the antenna prototype. A quick-fix ceramic material is fixed over the substrate. The optimized dimensions of the proposed filtenna are given in the caption of Fig. 1.

Step-by-Step Analysis of Proposed Radiator

To understand the physical properties of the proposed antenna, the design is divided into three steps: antenna-1 (circular patch along with conformal strip-loaded cylindrical DRA), antenna-2 (circular aperture-loaded cylindrical DRA) and the proposed antenna (combination of antenna-1 and antenna-2). A pictorial representation of all three antenna designs is displayed in Fig. 3.

Antenna-1 Analysis

The |S11| variation in antenna-1 is displayed in Fig. 4 with the variation in the radius of the circular patch. It can be observed that two resonance peaks are obtained at 2.5 GHz

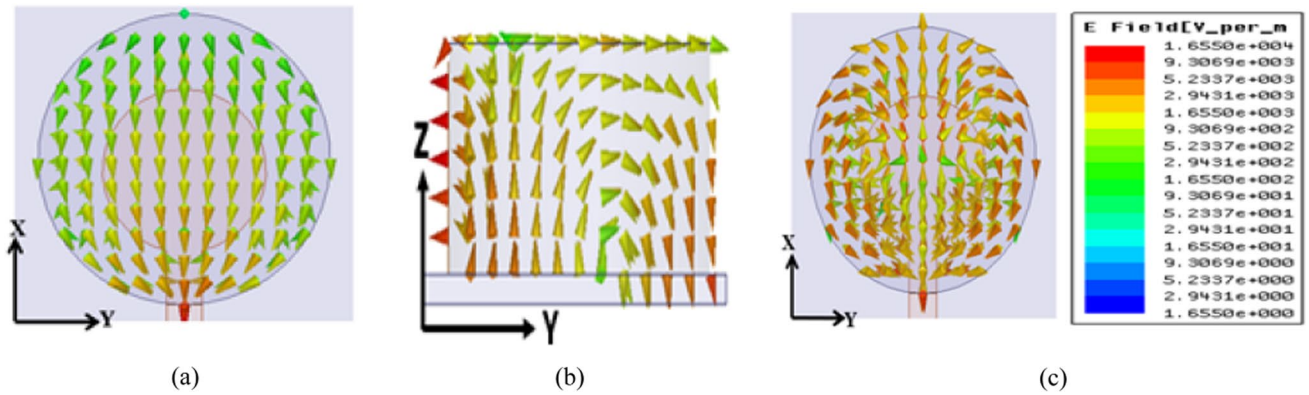

Fig. 5 Electric field variation on cylindrical ceramic at (a) 2.5 GHz, (b) 3.9 GHz, (c) 5.5 GHz.

and 5.5 GHz. As the radius of the circular patch increases, an additional resonance appears at 3.9 GHz, due to the high current density at the edges of the circular patch,[10] which affects the radiation characteristics of the fundamental mode. Therefore, R=7.0 mm is taken as the optimum value of the circular patch.

Figure 5 shows the electric field (E-field) rotation inside the cylindrical ceramic at resonance peaks 2.5 GHz, 3.9 GHz and 5.5 GHz, respectively. It can be seen that three different hybrid modes, $HEM_{11\delta}$, $HEM_{11\delta}$-like and $HEM_{12\delta}$ modes, are obtained at 2.5 GHz, 3.9 GHz and 5.5 GHz, respectively.[11] The $HEM_{11\delta}$ mode is created by the conformal strip, which acts as a magnetic dipole.[12] Similarly, a small current sheet maintains the horizontal field component uninterrupted and produces the $HEM_{12\delta}$ mode.[10] At 3.9 GHz, the E-field orientation of the $HEM_{11\delta}$ mode is disturbed due to high current density at the edges of the circular patch.[10] Hence, this mode is denoted as the $HEM_{11\delta}$-like mode.

Antenna-2 Analysis

Figure 6 shows the variation in |S11| of antenna-2 due to the change in the radius of the aperture (R_a). It is observed that three resonances again appear at 2.8 GHz, 4.2 GHz and 5.8 GHz.

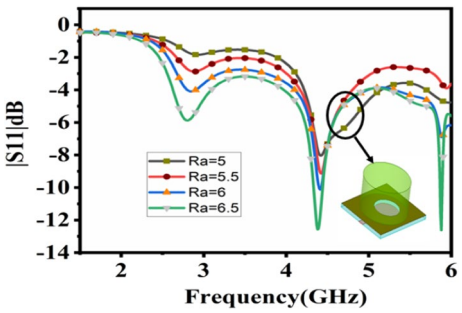

Fig. 6 |S11| variation due to change in radius of circular aperture (R_a).

In order to determine what is responsible for all of these resonances, the variation in the E-field on the DRA is displayed in Fig. 7. It can be seen that $HEM_{11\delta}$, $HEM_{11\delta}$-like and $HEM_{12\delta}$ modes are created at 2.8 GHz, 4.2 GHz and 5.8 GHz, respectively.[11] The circular aperture is able to create both orthogonal hybrid modes $HEM_{11\delta}$ and $HEM_{12\delta}$.[11] As the radius of the aperture increases, the impedance matching at 4.2 GHz ($HEM_{11\delta}$-like mode) improves, again because of the high current density at the edges of the aperture. However, this is not good for the radiator, because it affects the characteristics of the fundamental mode. Therefore, the optimized value of R_a is taken as 5.5 mm. One can also observe from Figs. 4 and 6 that the resonances due to aperture-coupled DRA are slightly shifted to the upper frequency. This is because of the reduction in the effective permittivity of the radiator.

Antenna-3 Analysis

Figure 8 displays the |S11| variation with antenna-1, antenna-2 and the proposed antenna (combination of antenna-1 and antenna-2). It can be seen that two frequency bands are obtained in the proposed antenna, i.e. 2.8 GHz and 5.5 GHz, which are due to the $HEM_{11\delta}$ mode and $HEM_{12\delta}$ mode, respectively. However, the resonance appearing due to the $HEM_{11\delta}$-like mode is suppressed in the case of the proposed antenna.

The variation in the gain in the lower and upper frequency bands is presented in Fig. 9a and b, respectively, due to changes in the radius of the circular metallic patch. Two important points are observed: (i) the gain in the operating band (lower and upper) is nearly 5.0 dBi, and (ii) the change in the radius of the circular patch directly affects the rejection value at 5.8 GHz and 3.5 GHz. Gain rejection at 5.8 GHz and 3.5 GHz occurs because of the creation

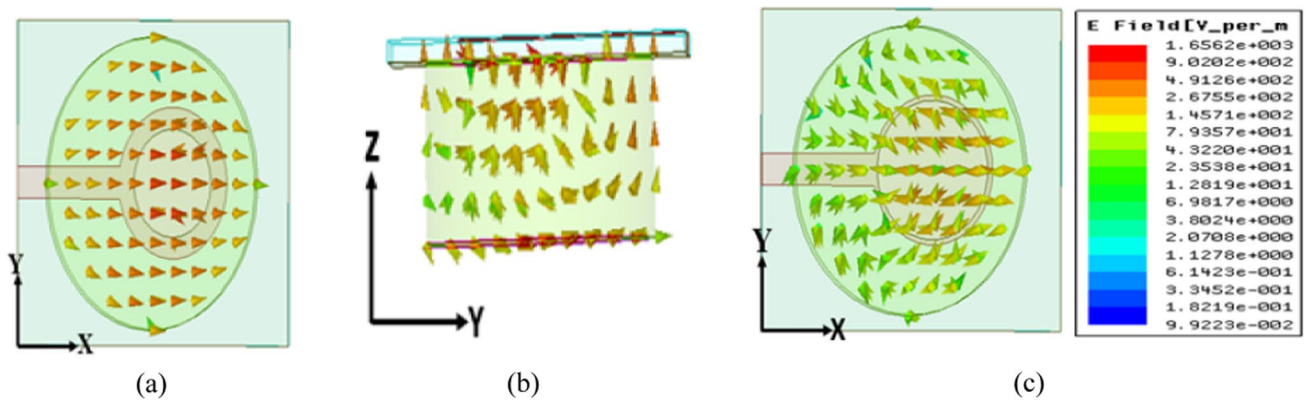

Fig. 7 Electric-field variation in the cylindrical ceramic at (a) 2.8 GHz, (b) 4.2 GHz, (c) 5.8 GHz.

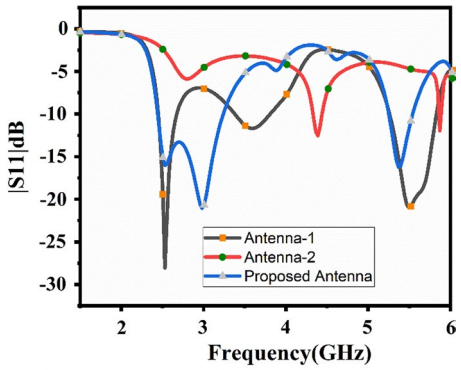

Fig. 8 |S11| variation with antenna-1, antenna-2 and proposed antenna.

of the radiation null. In the case of the proposed antenna, the upper cylindrical ceramic is excited using a dual signal transmission route, i.e. conformal strip along with the circular metallic patch. This dual-signal transmission approach for the dielectric resonator creates equal amplitude field lines with a 180° phase shift.

This produces the cross coupling, which introduces the radiation null at 5.8 GHz and 3.5 GHz.[6] In order to prove the aforementioned statement, Fig. 10 shows the E-field rotation at 3.5 GHz and 5.8 GHz. It can be observed that the E-field lines are aligned 180° out of phase and cancel each other, which in turn produces the radiation null. Figure 11a and b show the variation in gain in both frequency bands due to changes in the radius of the circular aperture. It is observed that the variation in the radius of the circular aperture directly affects the lower rejection value in both operating bands. The gain rejection at 2.0 GHz and 4.8 GHz is again due to the creation of the radiation null.

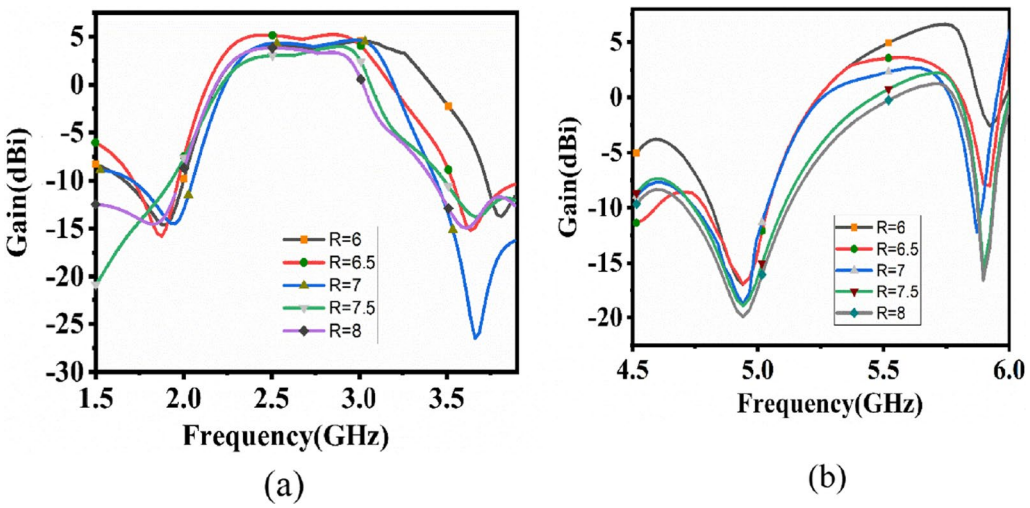

Fig. 9 Gain variation with change in radius of circular patch: (a) lower frequency band, (b) upper frequency band.

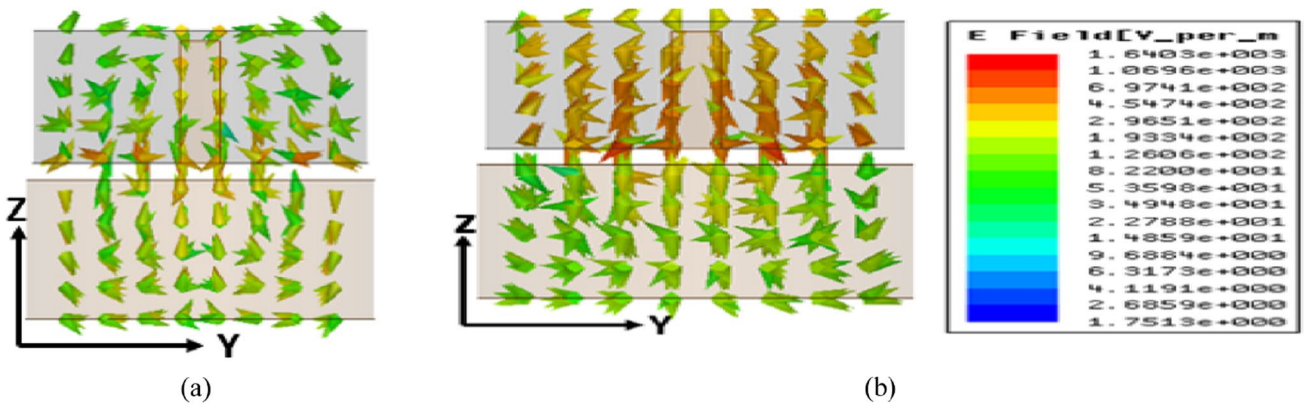

Fig. 10 Rotation of E-field on proposed antenna at (a) 3.5 GHz, (b) 5.8 GHz.

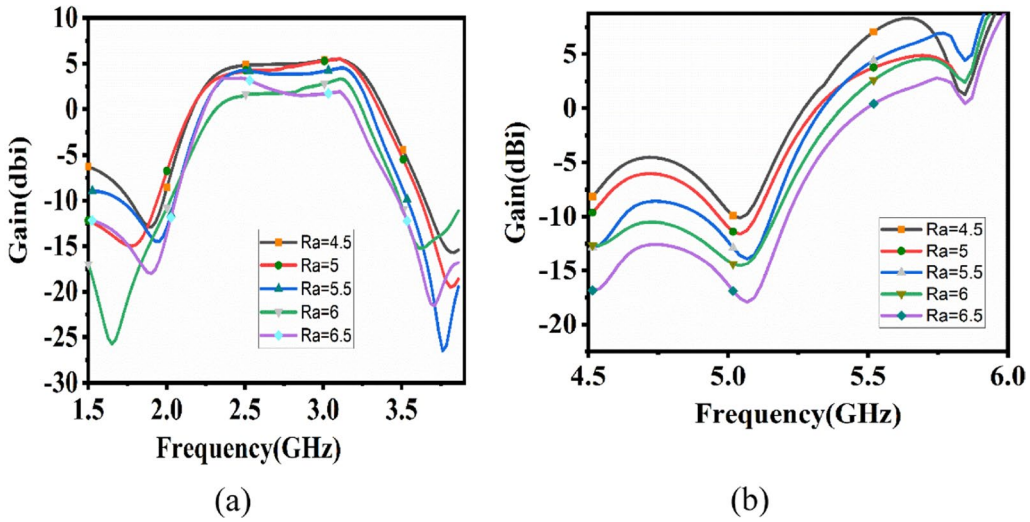

Fig. 11 Gain variation due to change in radius of circular aperture: (a) lower frequency band, (b) upper frequency band.

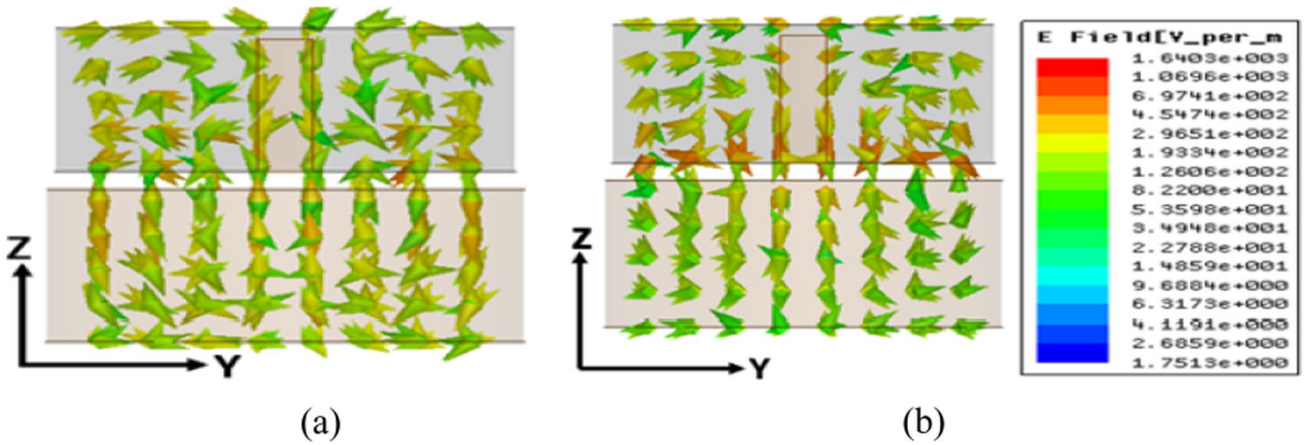

Fig. 12 Rotation of E-field on proposed antenna at (a) 3.5 GHz, (b) 5.8 GHz.

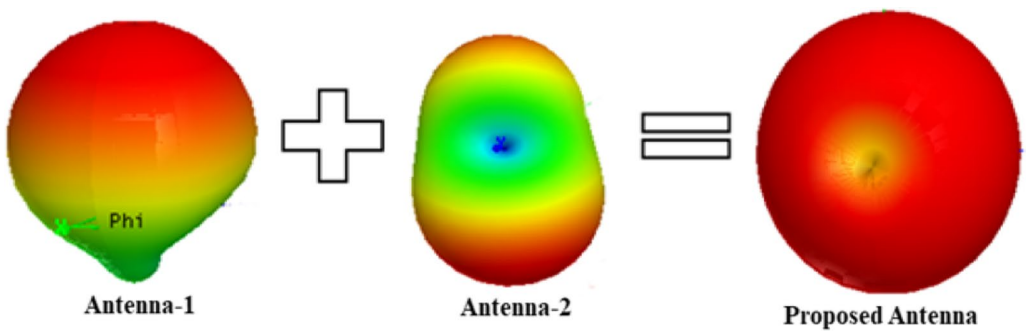

Fig. 13 3D far-field radiation pattern for different antennas at 2.8 GH.z.

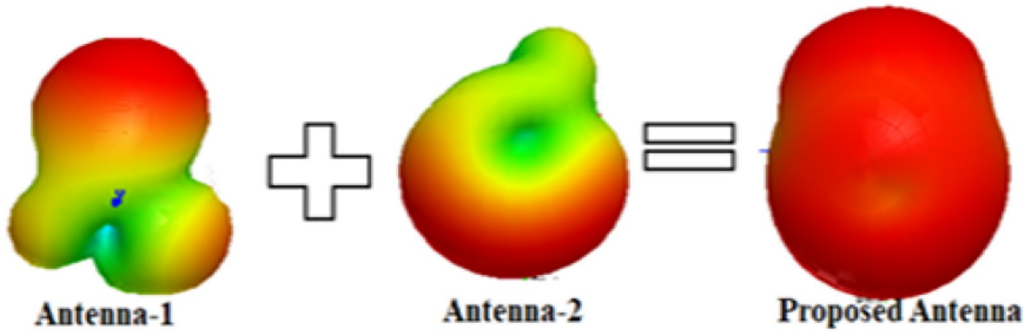

Fig. 14 3D far-field radiation pattern for different antennas at 5.5 GHz.

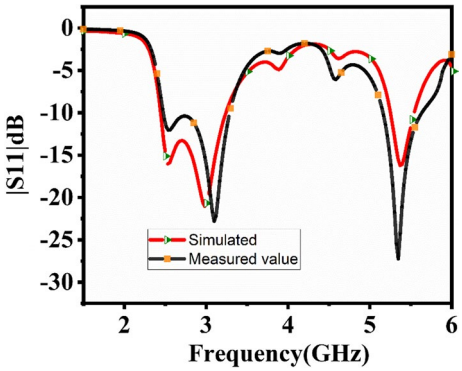

Fig. 15 Measured and simulated |S11| of proposed quasi-isotropic filtenna.

This radiation null is due to the combined effect of the aperture and circular patch on the upper side. Figure 12 shows the E-field rotation at 2.0 GHz and 4.8 GHz, which confirms that the E-field lines are 180° out of phase and cancel each other, which in turn produces the radiation null.

Another important feature of the designed antenna is the creation of a quasi-isotropic radiation pattern. Two concepts are integrated to achieve a quasi-isotropic radiation pattern in the proposed antenna: (i) two ceramic radiators are placed in opposite directions, i.e. antenna-1 and antenna-2, and (ii) both the $HEM_{11\delta}$ and $HEM_{12\delta}$ modes are supported in the ceramic material, which can create a broadsided radiation pattern.[12] When both antennas are combined in the proposed antenna, a quasi-isotropic radiation pattern is obtained. Figures 13 and 14 display the 3D radiation patterns of radiator-1, radiator-2 and the proposed radiator at 2.8 and 5.5 GHz, respectively. It can be clearly seen from Figs. 13 and 14 that antenna-1 and antenna-2 are radiating in the +Z direction and −Z direction, respectively. In the case of the proposed antenna, a quasi-isotropic radiation pattern is obtained.

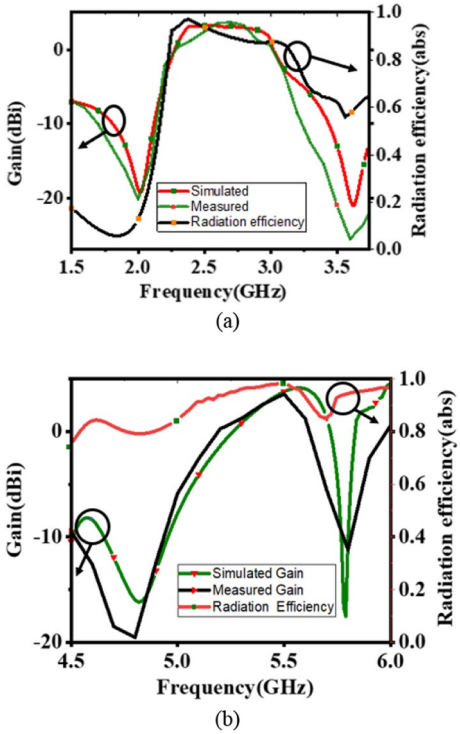

Fig. 16 Simulated and measured antenna gain of proposed quasi-isotropic filtenna. (a) Lower frequency band, (b) upper-frequency band.

Measured Outcome and Performance Comparison

In this section, the simulated results are verified by the measured outcome with the assistance of the antenna prototype (shown in Fig. 2). Figure 15 presents the measured and simulated values of the |S11| parameter of the proposed antenna. The reflection coefficient (|S11|) value is measured with a

Keysight E5071C ENA vector network analyzer (VNA). The measured and simulated values of |S11| are very similar.

Therefore, there is good agreement between the measured and simulated results. From Fig. 15, it is confirmed that the designed antenna works in dual bands, i.e. 2.48–3.3 GHz and 5.21–5.48 GHz. Figure 16a and b show the variation in measured and simulated results for antenna gain and radiation efficiency in the lower and upper frequency bands. Antenna gain is measured with the two-antenna method.[13] There is good agreement between the simulated and measured gain values. The maximum gain and radiation efficiency are around 5.0 dBi and greater

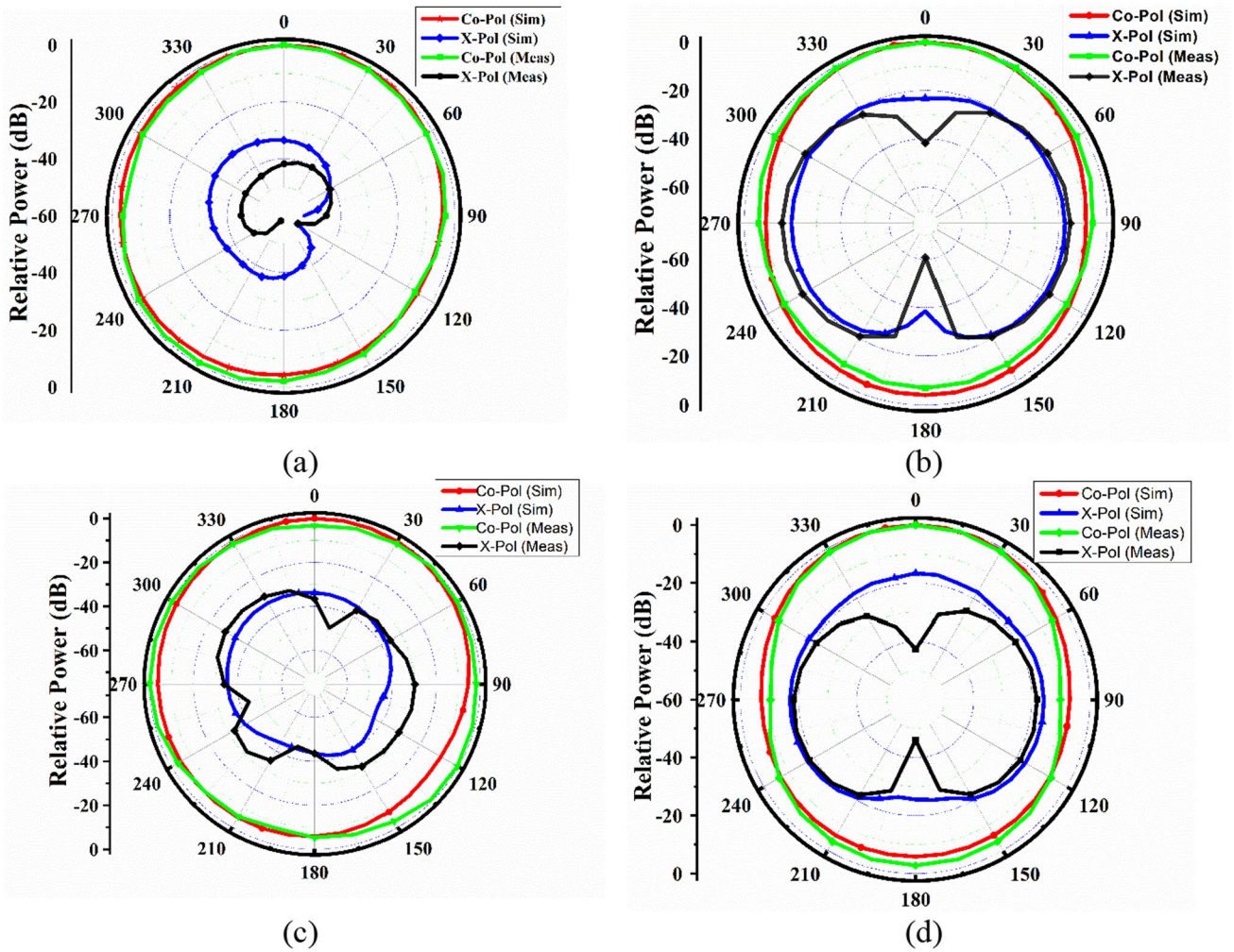

Fig. 17 Measured and simulated far-field radiation patterns of proposed quasi-isotropic filtenna: (a) XZ plane at 2.8 GHz, (b) YZ plane at 2.8 GHz, (c) XZ plane at 5.3 GHz, (d) YZ plane at 5.3 GHz.

Table I Comparison of proposed antenna with existing ceramic-based antennas

Antenna design	Operating frequency band	Filtering response (rejection in dB)	Quasi-isotropic radiation pattern
Cylindrical ceramic with cavity[5]	1.97–2.18 GHz (10.1%) and 3.42–3.55 GHz (3.73%)	Dual-band filtering response (rejection around 15 dB)	NA
Rectangular ceramic[6]	1.75–2.18 GHz (21.9%)	Single-band filtering response (rejection around 16 dB)	NA
Cylindrical ceramic[8]	2.38–2.55 GHz (6.9%)	NA	Yes (single band)
Cylindrical ceramic[9]	2.3–2.55 GHz (10.30%)	Single-band filtering response (rejection around 15 dB)	Yes (single band)
Proposed antenna	2.48–3.3 GHz (28.37%) and 5.21–5.48 GHz (5.05%)	Dual-band filtering response (rejection around 20 dB)	Yes (dual band)

than 90% within the operating frequency band. The value of gain rejection is around −20 dBi just outside the operating band due to the creation of the radiation null.

Figure 17 presents the far-field pattern in different planes (XZ and YZ) at 2.8 GHz and 5.3 GHz, respectively. Observation shows a good correlation between the simulated and measured far-field pattern. In both principal planes, the proposed antenna produces an omnidirectional radiation pattern. Therefore, the proposed antenna behaves as a quasi-isotropic antenna in both frequency bands. A large gap of around 20 dB exists between the co-polarization and cross-polarization levels, which attests to the good performance of the designed radiator. Table I provides a comparison of the proposed antenna with existing ceramic-based radiators. It can be seen that the proposed antenna is the first to provide a quasi-isotropic filtering response in the dual-frequency band.

Conclusion

In this work, a dual-band cylindrical ceramic radiator with both quasi-isotropic radiation features and filtering response is obtained. The quasi-isotropic radiation pattern is produced by combining the radiation patterns of the $HEM_{11\delta}$ and $HEM_{12\delta}$ modes obtained from antenna-1 and antenna-2 at 3.0 GHz and 5.4 GHz, respectively. Filtering characteristics are obtained by using an antenna fusion approach. The feeding mechanism, i.e. the combination of the microstrip line along with the conformal strip and circular aperture, produces four controllable radiation nulls at 2.0 GHz, 3.5 GHz, 4.8 GHz and 5.8 GHz, just outside the passband. Based on these results, the proposed radiator can be utilized in both wireless local area network (WLAN; 2.5 GHz/5.15 GHz) and IoT applications.

Authors' contributions Conceptualization and Methodology [Abhimanyu Yadav]; Writing—revised draft preparation: [Manish Tiwari]; Analysis and Investigation: [Abhimanyu Yadav and Anand Sharma]; Writing—original draft preparation and Supervision: [Anand Sharma].

Funding Author Anand Sharma wishes to acknowledge the Council of Science and Technology, U.P., for providing the financial support to successfully conduct this work (notification no. CST/D-2396 dated 24/03/2021).

Availability of data and materials Not applicable.

Conflicts of interest There are no potential conflicts of interest.

Ethics approval and consent to participate Not applicable.

Consent for publication I, Anand Sharma, give my consent for the publication of identifiable details, which can include photograph(s) and/or videos and/or figures and/or details within the text ("Material") to be published in the above Journal and Article.

References

1. Z.N. Chen, X.M. Qing, T.S.P. See, and W.K. Toh, Antennas for WiFi connectivity. *Proc. IEEE* 100, 2322 (2012).
2. Y. Yusuf, H.T. Cheng, and X. Gong, A seamless integration of 3-D vertical filters with highly efficient slot antennas. *IEEE Trans. Antennas Propag.* 59, 4016 (2011).
3. K. Dhwaj, J.M. Kovitz, H.Z. Tian, L.J. Jiang, and T. Itoh, Half-mode cavity based planar filtering antenna with controllable transmission zeroes. *IEEE Antennas Wirel. Propag. Lett.* 17, 833 (2018).
4. C.X. Mao, S. Gao, Y. Wang, and B. Sanz-Izquierdo, Dual-band patch antenna with filtering performance and harmonic suppression. *IEEE Trans. Antennas Propag.* 64, 4074 (2016).
5. P.F. Hu, Y.M. Pan, K.W. Leung, and X.Y. Zhang, Wide-/dual-band omnidirectional filtering dielectric resonator antennas. *IEEE Trans. Antennas Propag.* 66, 2622 (2018).
6. Y.M. Pan, P.F. Hu, K.W. Leung, and X.Y. Zhang, Compact single-/dual-polarized filtering dielectric resonator antennas. *IEEE Trans. Antennas Propag.* 66, 4474 (2018).
7. Z. Zhang, X. Gao, W. Chen, Z. Feng, and M.F. Iskander, Study of conformal switchable antenna system on cylindrical surface for isotropic coverage. *IEEE Trans. Antennas Propag.* 59, 776 (2011).
8. Y.M. Pan, K.W. Leung, and K. Lu, Compact quasi-isotropic dielectric resonator antenna with small ground plane. *IEEE Trans. Antennas Propag.* 62, 577 (2014).
9. P.F. Hu, Y.M. Pan, X.Y. Zhang, and B.J. Hu, A compact quasi-isotropic dielectric resonator antenna with filtering response. *IEEE Trans. Antennas Propag.* 67, 1294 (2019).
10. D. Guha, A. Banerjee, C. Kumar, and Y.M.M. Antar, Higher order mode excitation for high-gain broadside radiation from cylindrical dielectric resonator antennas. *IEEE Trans. Antennas Propag.* 60, 71 (2012).
11. A. Sharma, S. Gupta, G. Das, and R.K. Gangwar, Quad band quad sense circularly polarized dielectric resonator antenna for GPS/CNSS/WLAN/WiMAX applications. *IEEE Antenna Wave Propag. Lett.* 19, 403 (2020).
12. R.K. Mongia and P. Bhartia, Dielectric resonator antennas-a review and general design relations for resonant frequency and bandwidth. *Int. J. Microw. Millimeter-wave Comput. Aided Eng.* 4, 230 (1994).
13. W.L. Stutzman and G.A. Thiele, *Antenna theory and design* (NJ: A JohnWiley & Sons; Hoboken, 2013).